Received: 17 February 2022 | Accepted: 14 May 2022

DOI: 10.1002/ajb2.16000

RESEARCH ARTICLE

Botany

Holding on or falling off: The attachment mechanism of epiphytic *Anthurium obtusum* changes with substrate roughness

Jessica Y. L. Tay[1] | **Alexander Kovalev**[2] | **Gerhard Zotz**[1,3] | **Helena J. R. Einzmann**[1] | **Stanislav N. Gorb**[2]

[1]Functional Ecology of Plants, Institute of Biology and Environmental Sciences, University of Oldenburg, P.O. Box 2503, D-26111 Oldenburg, Germany

[2]Functional Morphology and Biomechanics, Zoological Institute, Kiel University, Am Botanischen Garten 9, 24118 Kiel, Germany

[3]Smithsonian Tropical Research Institute, Balboa, Panama, Republic of Panama

Correspondence

Jessica Y. L. Tay, Functional Ecology of Plants, Institute of Biology and Environmental Sciences, University of Oldenburg, P.O. Box 2503, D-26111 Oldenburg, Germany.
Email: jessica.tay.ying.ling@uol.de

Abstract

Premise: For vascular epiphytes, secure attachment to their hosts is vital for survival. Yet studies detailing the adhesion mechanism of epiphytes to their substrate are scarce. Examination of the root hair–substrate interface is essential to understand the attachment mechanism of epiphytes to their substrate. This study also investigated how substrate microroughness relates to the root–substrate attachment strength and the underlying mechanism(s).

Methods: Seeds of *Anthurium obtusum* were germinated, and seedlings were transferred onto substrates made of epoxy resin with different defined roughness. After 2 months of growth, roots that adhered to the resin tiles were subjected to anchorage tests, and root hair morphology at different roughness levels was analyzed using light and cryo scanning electron microscopy.

Results: The highest maximum peeling force was recorded on the smooth surface (glass replica, 0 µm). Maximum peeling force was significantly higher on fine roughness (0, 0.3, 12 µm) than on coarse (162 µm). Root hair morphology varied according to the roughness of the substrate. On smoother surfaces, root hairs were flattened to achieve large surface contact with the substrate. Attachment was mainly by adhesion with the presence of a glue-like substance. On coarser surfaces, root hairs were tubular and conformed to spaces between the asperities on the surface. Attachment was mainly via mechanical interlocking of root hairs and substrate.

Conclusions: This study demonstrates for the first time that the attachment mechanism of epiphytes varies depending on substrate microtopography, which is important for understanding epiphyte attachment on natural substrates varying in roughness.

KEYWORDS

anchorage strength, bio-adhesion, epiphytes, glue-like substance, mechanical interlocking, root hairs

The typical root system of a vascular plant serves important functions such as water and nutrient uptake, as well as providing vital anchorage and support to the plant. Anchorage has been studied for the root systems of seedlings to adult trees (e.g., Ennos, 1989, 1990, 2000; Blackwell et al., 1990; Crook and Ennos, 1996; Nicoll et al., 2006). Additionally, others have examined how external mechanical loadings on the shoots are transmitted to the root system for stability and effective anchorage (e.g., Coutts, 1986; Gartner, 1994; Nicoll and Ray, 1996; Stokes and Guitard, 1997; Peltola et al., 2000). Having a stable anchorage is important for survival against external mechanical stresses such as wind (wind throw) (e.g., Stokes, 1999; Mickovski and Ennos, 2003; Fournier et al., 2006). Effective anchorage depends largely on the mechanical properties of the roots and the overall root architecture (i.e., rooting depth, root plate width, root branching; e.g., Warren et al., 1988; Ennos, 1993; Crook et al., 1997; Fourcaud et al., 2003; Di Iorio et al., 2004; Dupuy

et al., 2007; Štofko and Kodrik, 2008). Studies on root anchorage mainly focused on plants that are rooted in terrestrial soil, but surprisingly, very rarely on vascular epiphytes, a lifeform where plants stay permanently attached to their host via their roots.

Vascular epiphytes (hereafter, referred to as epiphytes) represent an extremely species-rich group of plants, mainly occurring in the tropical and subtropical forest ecosystems. They make up more than 31,000 species, representing almost 10% of the global vascular plant diversity (Zotz et al., 2021b). Epiphytes are, by definition, nonparasitic to their host trees, but are structurally dependent on them. This lifeform provides an opportunity for epiphytes to colonize spaces in the canopy such as in tree crotches filled with organic materials or arboreal soil in the montane environment (Hoeber et al., 2019), main trunk and branches covered with humus or moss mats (Van Leerdam et al., 1990), and on "bare" twigs that are not covered with organic materials (Rudolph et al., 1998). Secure attachment to their host is vital for the survival of epiphytes (Rodríguez-Robles et al., 1990; Tremblay, 2008), because their chances of survival on the ground are low (Matelson et al., 1993). Their root systems differ from the typical fibrous, tap, or plate root systems of terrestrial plants (i.e., Coutts, 1983; Ennos and Fitter, 1992; Ennos, 2000). As mentioned above, some epiphytes root on bare twigs, directly on the bark without any organic materials (Appendix S1). For these so-called bark epiphytes (Zotz, 2016), roots grow fully exposed on the surface of the substrate. These roots do not penetrate the host's tissues (unlike parasitic mistletoe roots), but instead achieve attachment to their host by maximizing the area of contact with the substrate (Tay et al., 2021), or by mechanical interlocking with the dead bark tissues. To resist dislodgement of the epiphyte from the host, these roots have to withstand a considerable amount of mechanical loading, including (1) the weight of the epiphyte (self-loading), (2) in the case of tank bromeliads—additional impounded water and organic material in the tank (Brandt et al., 2017; Zotz et al., 2020), and (3) external forces such as wind and rain (Telewski, 1995; Tay et al., 2022).

To date, studies detailing the biological adhesion mechanisms of plant roots to their substrate mainly focused on climbers and seagrasses (Isnard and Silk, 2009; Yang and Deng, 2017; Zenone et al., 2020a). For example, Melzer et al. (2011) provided an in-depth investigation of the attachment mechanism of the root climber English ivy, *Hedera helix*, which uses a combination of glue secreted from the root and a subsequent shape change of the root hairs to secure its hold to the substrate. In the seagrass *Posidonia oceanica*, attachment to hard rock substrates could result from the combination of glue-like substance from the roots, mechanical interlocking of root hairs to the substrate and, possibly, suction force from the attachment pads formed at the root tips (Badalamenti et al., 2015; Borovec and Vohník, 2018; Zenone et al., 2020a). Steinbrecher et al. (2010) and Zenone et al. (2020a) went a step further from microscopic analyses of the root structures to quantitatively define the mechanical strength of the root–substrate attachment. For example, a 2-cm internodal root segment of *Hedera helix* attached to tree bark had a maximum attachment strength of 7 N; while the maximum attachment strength of the nodal attachment roots of the trumpet vine *Campsis radicans* to birch wood was 25 N (Steinbrecher et al., 2011). Finally, Zenone et al. (2020a) noted that the root attachment strength of seagrasses is a function of substrate roughness, where 12 μm seemed to be the optimal substrate roughness for the strongest attachment of 2.5 N. The observation that substrate roughness affects the root attachment mechanism and its strength was the starting point for the present study.

Only a few studies implicitly explored the attachment mechanism of epiphytic plants to their substrate. Orchids, aroids, and bromeliads have noticeable root hairs that emerge only from the side of the root that is in direct contact with the substrate (Dycus and Knudson, 1957; Benzing, 1970; Brighigna et al., 1990; Mathews et al., 1997; Stern and Judd, 1999; Stern, 2014; Ponert et al., 2016; Muthukumar and Kowsalya, 2017; Deseo et al., 2020). Root hairs of an epiphytic orchid were observed to enter microcrevices on the substrate surface, providing some degree of interlocking mechanism between the root and substrate (Tay et al., 2021), contributing to the overall anchoring strength of the plant to its host. However, the mechanical attachment of epiphytes to their hosts has received little scientific attention and usually discussed in relation to bark properties such as rugosity and substrate stability. For example, trees with flaky or peeling bark should be poor hosts since the plants may fall off with the unstable substrate (e.g., Steege and Cornelissen, 1989; Hietz and Hietz-Seifert, 1995; Malizia, 2003; Wyse and Burns, 2011). In contrast, trees with more rugose bark may be better hosts since there are more crevices for roots to enter, contributing to anchorage of the whole plant (e.g., Callaway et al., 2002; Malizia, 2003). It has been noted early on that roughness is important for epiphyte establishment and growth (Schimper, 1888; Oliver, 1930; Went, 1940); however, there is no protocol to define bark roughness, and diverse methods have been applied. For example, bark roughness was assessed visually (Adhikari et al., 2012; Ceballos et al., 2016), in terms of furrow depth and width on the bark (Lewis and Ellis, 2010) or by means of folding a thin cotton thread to conform to every asperity and crevice over a certain length of the bark (Callaway et al., 2002). However, it is questionable whether the scale at which roughness is studied so far is relevant (Zotz et al., 2021a). More specifically, there is still a lack of understanding regarding how the roots interact with their host substrate: What is the attachment mechanism of epiphytic roots to their substrate? Without this basic knowledge, correlating arbitrarily defined "bark rugosity" with epiphyte density can be highly misleading. A surface has multiple scales in nature and the implied roughness of the surface is based on how close-up the surface is examined. Therefore, the rugosity of a surface can be measured on the millimeter, micrometer and nanometer scales, depending on how root attachment is understood and defined. For example, on deeply fissured bark (i.e., centimeter and millimeter scales),

the entire root of the epiphyte often grows directly into the furrows (J. Y. L. Tay, personal observations). When the root is jammed tightly into grooves of the bark, a large area of the root is in direct with the substrate, which could in turn strengthen the attachment of the plant to the tree. The recent study by Tay et al. (2021) found that on a relatively smooth bark substrate, the mechanics of attachment for epiphytic orchids occurs at the scale of the root hair–substrate interface where the actual contact area is defined (see fig. 6 of Tay et al., 2021). Therefore, the concept of rugosity in terms of how it is measured and how it relates to epiphyte abundance and richness should be discussed based on how attachment is defined in the first place. Nonetheless, as a starting point, the present study will investigate substrate roughness on the microscale, focusing on the contact area between the root hair and substrate.

Here, we aimed to shed light on the role of substrate microroughness on the root–substrate attachment mechanism and strength. A greenhouse experiment was designed to systematically investigate the adhering roots of an epiphytic aroid, *Anthurium obtusum*. Seedlings were grown on artificial substrate tiles made of epoxy resin with different levels of well-defined roughness. The objectives of this study were to (1) analyze the root anchorage strength (via peeling and shear tests) and (2) investigate how root hair morphology changes (using light microscopy and cryogenic scanning electron microscopy [Cyro-SEM]), when the plant was in contact to substrate with different microroughness. We hypothesized that the mechanism, through which root hairs adhere to the substrate, changes, depending on the magnitude of roughness, which in turn should influence the attachment strength of the root. Root hair attachment would be mainly via mechanical interlocking with an increasing degree of roughness of the substrate surface. On less rough surfaces, root hairs are most likely to adapt well to the topography of the substrate and achieve a large contact area, thus demonstrating a strong attachment mechanism. Given a highly "rugged and bumpy" substrate, root hairs will be limited in terms of length and will not be able to adapt to the substrate surface, to reach sufficient contact area. Thus, the overall attachment mechanism should be presumably weak, but it might be additionally enhanced by stronger mechanical interlocking between root hairs and substrate corrugations.

MATERIALS AND METHODS

Seeds germination and sample preparation

Anthurium Schott is by far the most species-rich genus in the family Araceae, consisting of 1139 accepted species (WCSP, 2022), with 665 species described as epiphytes (Zotz et al., 2021b), one of which is *Anthurium obtusum*. In February 2021, 150 seeds, collected from mature fruits of this species from the greenhouse (University of Oldenburg, Germany), were germinated on damp paper towels in glass jars. These jars were placed in the greenhouse (Botanical Garden Kiel University, Germany) with a 12 h light/12 h dark photoperiod provided by natural light (15,000 to 25,000 lux), supplemented with a 400 W sodium discharge lamp, at 24°C. After 2 weeks, the resultant seedlings were transferred from the paper towels to Seramis granules (Seramis GmbH, Mogendorf, Germany) and were misted once a day. After another 2 weeks, most seedlings had one leaf and one root. These seedlings were then transferred to a greenhouse at the University of Oldenburg, Germany, that was better equipped to keep seedlings and substrate constantly moist. The greenhouse has climatic conditions similar to that of humid tropic conditions, with light values at 80 μmol m^{-2} s^{-1} in a 12/12 hr light/dark photoperiod. The light/dark temperature was 28/20°C, with relative humidity of 80/60%, respectively.

Surface roughness is defined by the particle sizes/height on the polishing and sandpapers used to create the artificial substrate. Epoxy resin tiles (4 × 4 cm) were prepared as substrate replicas of clean glass surface (no roughness, hereafter "smooth"), polishing paper (particle size 0.3 μm, Serva Electrophoresis GmbH, Heidelberg, Germany) and sandpaper (particle sizes 3, 12, 30, 68, and 162 μm, Starcke GmbH & Co. KG, Melle, Germany), for a total of seven roughness levels and 12 replicates per roughness level (total 84 tiles). The producers of the polishing and sandpapers provided the reported particle sizes. Tile preparation and roughness characterization was detailed by Zenone et al. (2020a). In total, 84 healthy seedlings were selected for attaching to the tiles. One seedling was laid on a tile and secured with a rubber band to ensure that the root remained in tight contact with the tile surface. These seedlings were left to grow in the greenhouse for 2 months (March to May 2021 at the University of Oldenburg, Germany). So that the seedlings were always moist, they were placed under the RELDAIR Fog system (Reldair, Oldenzaal, Netherlands), in which mist intervals depend on the humidity settings controlled by the humidity sensor. When the humidity goes below the set point, the fog system starts for a minimum of 2 min and maximum of 17 min. When the humidity is above the set point, then the roof windows open to ventilate the greenhouse. The positions of the resin tiles were manually randomized every week to eliminate any bias from light and water conditions (Appendix S2).

Anchorage strength measurement: peel and shear tests

At the end of the growing period (Appendix S3), 10 samples of each roughness level were used to measure the root anchorage strength to the substrate. The remaining two samples were used for morphological analysis with a light microscope and for Cryo-SEM imaging.

For measuring the attachment strength, roots that adhered to the tiles were cut from the main seedling body.

Measurements were recorded with a DS4 peeling tester (TETRA GmbH, Melle, Germany). One end of a nylon thread was tied to the cut end of the root (cut at the proximal end with a disposable razor blade), and the other end was fixed to the sensor of the tester. The sensor was positioned at 90° and 0° to the tile surface for the peel and shear test, respectively (Appendix S4). In a valid test, the machine pulled on the thread until the root was completely detached from the substrate (pulling speed = 0.1 mm/s; acceleration speed in the beginning = 5 mm/s^2), and the maximum force of attachment was recorded for each sample. Overall, there were 104 valid peel tests (at least 11 tests per roughness) and 39 shear tests (at least 4 tests per roughness).

Root hair morphology

Visibility of the attached root hairs on the resin surface was enhanced by staining the roots of the seedlings with methylene blue. Since the resin tiles are slightly translucent, with the seedling still attached to the tile, root hairs were observed from the underside of the tile using a light microscope (Zeiss Axioplan, AxioCam MRc, Carl Zeiss Microscopy GmbH, Jena, Germany). Resin tiles with fresh portions of the root still attached were cut into suitable sizes with a wire cutter, to be mounted on the stub for cryo-SEM examination. However, in the process of cutting the resin, roots were detached completely from some of the tiles, so that no root fragments were left on the resin for further examinations. Therefore, for substrates at the 0.3, 12, 68, and 162 µm roughness levels, there were no suitable samples available for cryo-SEM examinations. We acknowledge this caveat for the study. Nonetheless, root samples attached to the substrate with 0, 3, and 30 µm roughness levels were studied, thus providing a good range of substrate microroughness to examine any changes in root hair morphology. The mounted samples were shock-frozen (–140°C) in a Cryo-SEM Hitachi S-4800 (Hitachi High-Technologies Corp., Tokyo, Japan) equipped with a Gatan ALTO 2500 cryo-preparation system (Gatan Inc., Abingdon, UK). Then, samples were sputter-coated in frozen conditions with gold-palladium (thickness 10 nm) and examined at 3 kV acceleration voltage at –120°C in the microscope. High-resolution micrographs were obtained and used to visualize how root hairs interacted with the surface topography at the different microroughnesses of the substrates. To determine the thickness of the root hair cell walls, we imported relevant micrographs into Fiji, a distribution of ImageJ for image analysis (Schindelin et al., 2012).

Data analyses

Differences in the peeling and shear tests between the roughness levels were analyzed through a one-way ANOVA with the roughness factor fixed at seven levels (smooth, 0.3, 3, 12, 30, 68, and 162 µm). Data were log-transformed to meet the assumptions of the ANOVA, which were checked with the residuals versus fitted plot and the normal Q-Q plot. When a significant difference was found, a post hoc Tukey test was performed. Boxplots were used to visualize the results of the anchorage tests against different substrate roughness. All statistical analyses were performed in R (version 3.6.3; R Core Team, 2021).

RESULTS

Seedling growth

All seeds germinated within 1 week, and one primary root grew after germination. At the end of the 2-month growth period, 10% of the seedlings were not attached to the substrate, with a majority failing on the substrate with 30 µm roughness. The remaining seedlings that adhered to the resin tiles showed no significant morphological differences across the different roughness levels (one-way ANOVA, $P > 0.05$): on average, the seedlings had 2 ± 1 (mean ± SD) leaves, 3 ± 1 roots, with a mean root length of 1.8 ± 0.9 cm.

Root adhesion test

Roots adhered to substrates of all levels of roughness tested. At least 11 peel tests and four shear tests were successful at each roughness level (Figures 1 and 2). However, not all the roots on a seedling produced a successful anchorage, either because they had no attachment or were loosely attached to

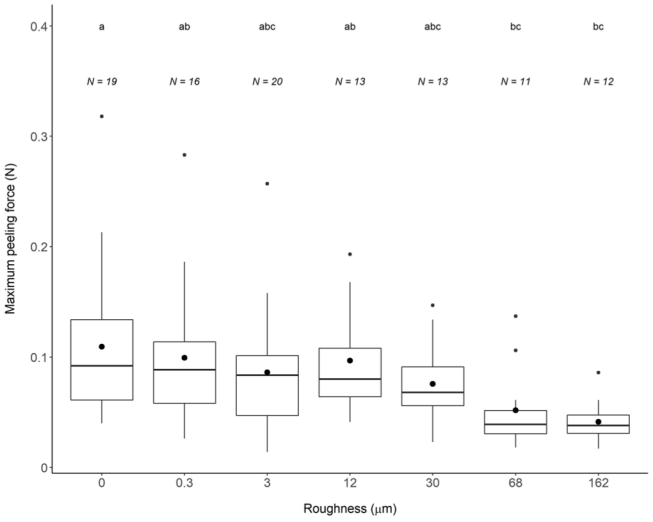

FIGURE 1 Peeling test of adhered roots to the resin substrate of increasing roughness. The sample size (*N*) for tested roots is given for each roughness level. The ends of the boxes define the 25th and 75th percentiles; the horizontal line at the median and error bars defines the 10th and 90th percentiles. The points inside the boxplots are means; the points outside the boxplots are outliers. Different lower-case letters indicate significant differences (post-hoc Tukey test, $P < 0.05$).

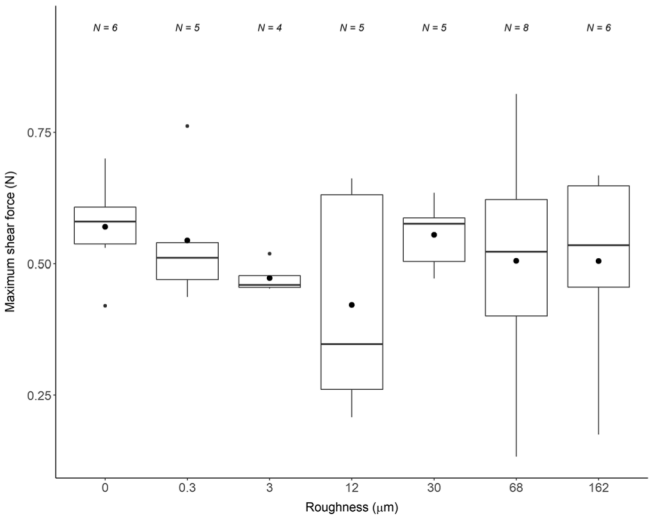

FIGURE 2 Shear test of attached roots to the resin substrate of increasing roughness. The sample size (*N*) for tested roots is given for each roughness level. The ends of the boxes define the 25th and 75th percentiles; the horizontal line at the median and error bars defines the 10th and 90th percentiles. The points inside the boxplots are means; the points outside the boxplot are outliers. Shear forces did not differ with roughness (Kruskal–Wallis test, $P > 0.05$).

the substrate. In the last case, the roots detached when they were cut from the seedling body or later, when the nylon thread was tied to them.

The mean maximum peeling force varied 2-fold from 0.05 ± 0.04 N on the 162 μm surface to 0.11 ± 0.07 N on the smooth surface (Figure 1). The highest maximum peeling force measured was 0.21 N, for a root on the smooth surface. There was a significant difference in the maximum peeling force with roughness level (one-way ANOVA, $F_{6,97} = 4.7$, $P < 0.001$). Maximum peeling force was significantly higher on the substrates 0 μm, 0.3 μm and 12 μm, as compared to the highest roughness of 162 μm, and comparing between 0 μm and 68 μm substrates (post-hoc Tukey test, $P_{(\text{max. peel force} \sim \text{roughness})} < 0.05$; Figure 1).

Variation in the mean maximum shear force was much lower, ranging from 0.42 ± 0.21 N on the 12 μm surface, to 0.57 ± 0.1 N on the smooth surface. The shear test data set did not meet the homogeneity of variance assumption required to carry out a one-way ANOVA. A Kruskal-Wallis test did not detect a significant difference in the maximum shear force between the levels of roughness ($P > 0.05$) (Figure 2).

Root hair morphology

The root hair morphology changed according to the roughness of the substrate. The figures show adhesion of the root hairs on substrates of increasing roughness, i.e., 0 μm (Figure 3), 3 μm (Figure 4), and 30 μm (Figure 5). On the smooth substrate, root hairs overlapped one another (Figure 3B, D, E, G), and root hairs adhered to the substrate (Figure 3B). Root hairs were mostly flattened over the substrate surface, with a large proportion of the root hairs in direct contact with the substrate (Figure 3B, G, H). The root hairs replicated the surfaces that they had adhered to, for example, the smooth surface of the resin (Figure 3B) and the outline of an overlapped root hair (Figure 3H). Some root hairs were also tubular-shaped, with only the bottom part of the root hairs adhering to the substrate (Figure 3A, C. D). On the substrate with 3 μm roughness, root hairs also overlapped one another and were flattened (Figure 4A), and a large area of the root hairs was in contact with the substrate. The root hairs clearly replicated the topography of the resin (Figure 4A); the microroughness of the substrate was clearly seen imprinted on the root hair (Figure 4B). As roughness increased to 30 μm, root hairs did not overlap each other. Root hairs were a mixture of flattened and tubular-shaped (Figure 5C, D); both forms conformed to the spaces between the asperities and contacted the substrate at multiple points (Figure 5C, D). The cell wall of the root hair was very thin (ca. 0.45 μm; Figure 5E).

When roots were stained with methylene blue, on the smoother surfaces, the contact between the root and resin was watertight, barely allowing the dye to stain the root hairs, resulting in a pale blue appearance (Appendix S5a). The rougher surfaces allowed the dye to stain the root hairs more easily, resulting in a dark blue appearance (Appendix S5b, c; Figure 6). At the highest roughness, 162 μm, many root hairs grew and elongated toward the resin surface, growing between the asperities (Figure 6A, B). The root hairs were tubular (Figure 6B) and wrapped around the asperities on the resin (Figure 6C).

Presence of "glue"

On the substrates with smooth or fine roughness, i.e., 0 μm and 3 μm, traces of an amorphous substance ("glue") were observed on the surface of the root hairs and at the interface between the root hairs and the resin surface (Figures 3E, F; 4C, D). This glue-like substance filled the gaps, forming a close contact between the root hairs and the substrate (Figure 3F). In one case, as the root hairs extended toward the resin surface, they appeared to be completely covered by an amorphous substance (Figure 4D, see root hair marked by white arrow). Similarly on the rougher substrate (30 μm), a glue-like substance was present, although not in the same quantity as observed on the smoother substrate. Glue-like substance was observed between the root hairs and the asperities on the resin surface, but only where contact was made (Figure 5C, E, F).

DISCUSSION

Hydrophobic properties of tree bark

This present study is the first to provide insights into how the strength of the root attachment of an epiphytic aroid

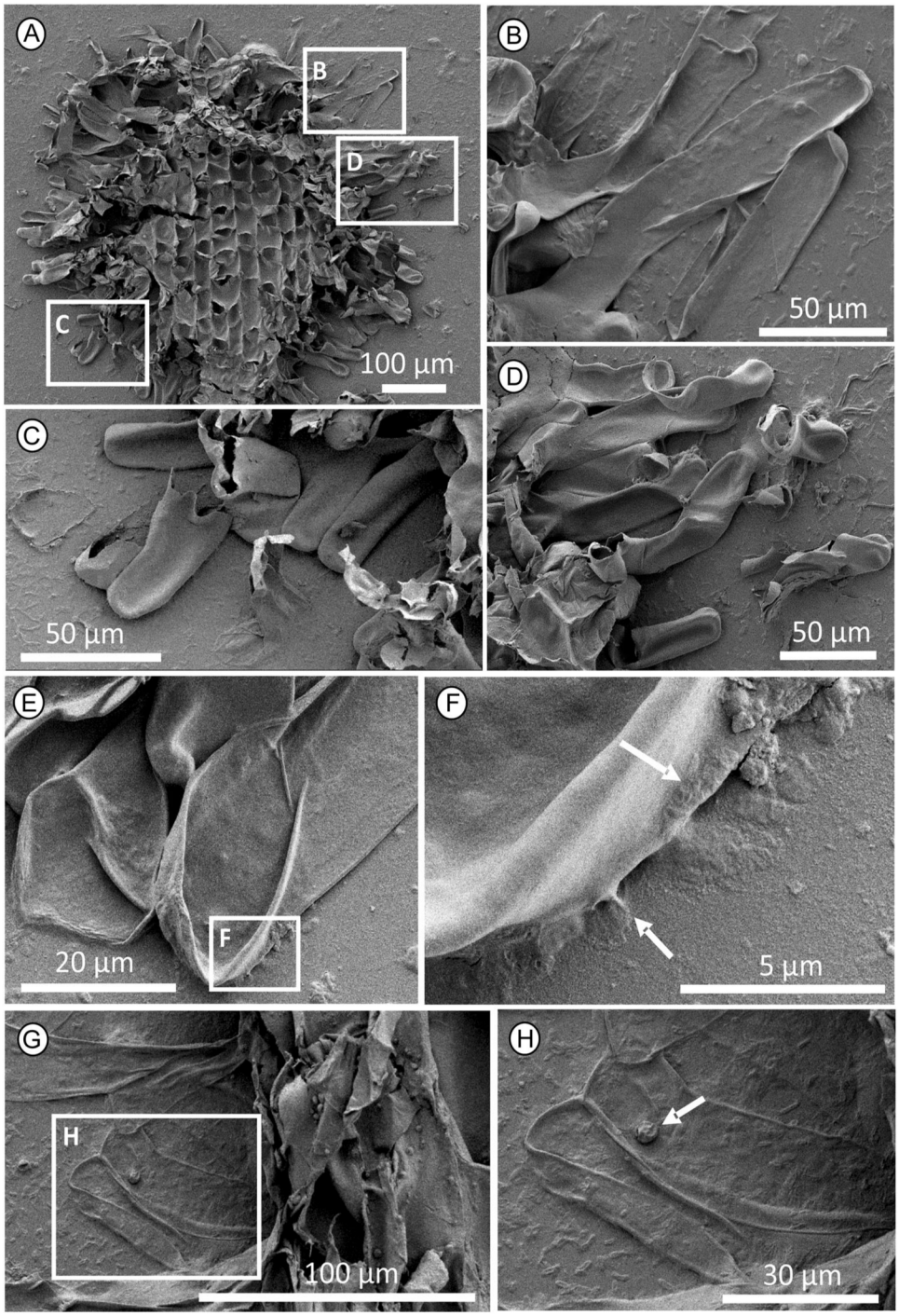

FIGURE 3 Cryo-SEM micrographs of *Anthurium obtusum* root with its root hairs adhering to the smooth resin surface (0 µm). (A) Overview of a piece of the root with the underside attached to the resin surface. Several root hairs emerged from the velamen layer and also adhered to the resin. (B–D) Close-up images of the root hair attachment to the resin. (B) Root hairs area completely flattened on the surface and have a large area of contact with the substrate. (C, D) Tubular root hairs that seem to adhere to the surface with a substance that left a mark on the resin when the root hair was removed (see C). (F) Enlargement of boxed area in (E). Root hairs adhere to the resin with a layer of an amorphous substance (glue) that is present on the root hair and on the resin surface (white arrows). (H) Enlargement of boxed area in (G). Flattened root hairs with a layer of substance growing over them. A single-celled green alga is on the surface of a root hair (white arrow).

depends on substrate microtopography. In preliminary experiments, seedlings were grown directly on microscope glass slides (VWR International GmbH, Darmstadt, Germany). However, the seedlings did not achieve any form of adhesion to the glass slides, in contrast to the resin replica of glass, to which the seedlings adhered strongly. This observation is interesting because it illustrates that material properties of the substrate also

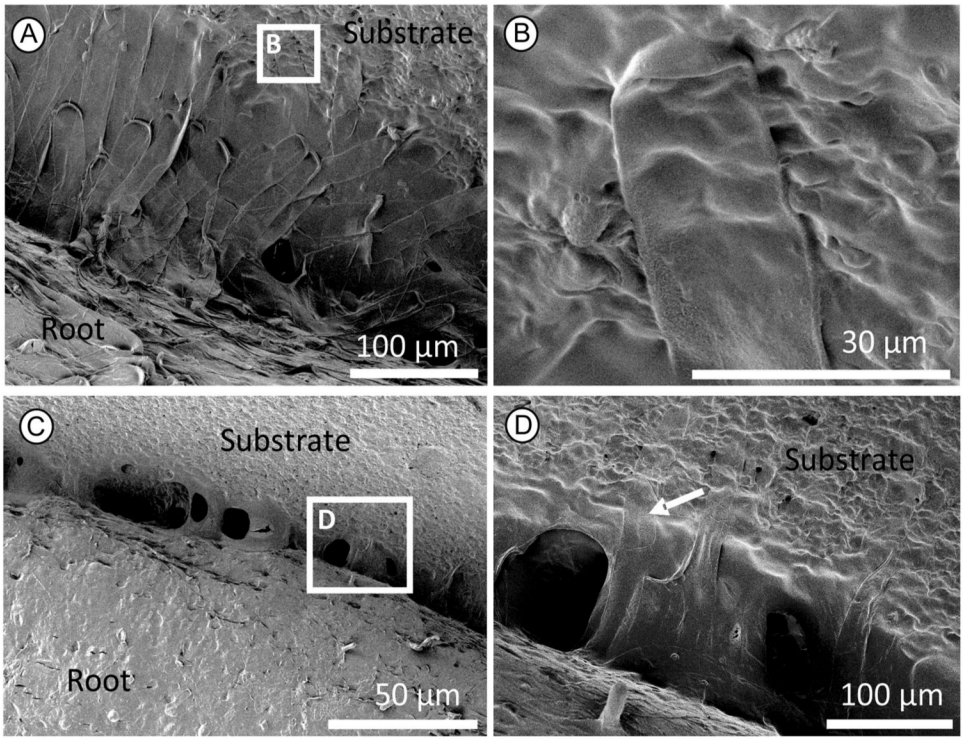

FIGURE 4 Cryo-SEM micrographs of *Anthurium obtusum* with its root hairs adhering to the resin of roughness 3 µm. (A) Numerous root hairs growing from the velamen layer and adhering to the resin surface. Root hairs overlapped one another. (B) Enlargement of boxed area in (A). A single root hair is adhering to the resin surface, and the microcontours of the resin are clearly replicated by the root hair, suggesting that root hair cell walls are very thin. (C) Part of the root adhered to the resin surface. There is a layer of an amorphous substance between the root hair and the resin. (D) Enlargement of boxed area in (C). Extension of root hairs onto the resin surface (white arrow). The gap between the main root and resin is clearly filled with a fluid like substance (glue).

play a role in the adhesion capacity of the roots. Microscope glass slides vary depending on the manufacturers. Those used in the experiment were hydrophilic; because of its high wettability, water spreads across the slide (Drelich et al., 2011). Tree bark is known to contain some hydrophobic substances, which can hinder water penetration (Borgin and Corbett, 1971; Borgin and Corbett, 1974; Passialis and Voulgaridis, 1999). This property is important to protect the tree from excessive loss of moisture, especially in hot and dry climates. The difference in the surface free energy between the glass slides and tree bark already hints at possible reasons for the failure to attach to glass surfaces. Additionally, when the epoxy resin (a type of thermosetting plastic) was used to produce our experimental surface, roots strongly attached to the smoothest substrate. In comparison to glass, resin is more hydrophobic (Voigt et al., 2011), and perhaps the material properties of epoxy resin are presumably closer to that of natural bark, hence promoting adhesion of the plant root hairs. In addition to the natural relief of the bark, the material and chemical properties of the substrate also seem to play a role to assist the adhesion of plant root hairs, but this topic is beyond the scope of our study.

Attachment mechanism of aroid root hairs

When seedlings of *Anthurium obtusum* were grown on artificial substrates ranging from smooth (0 µm; Ra ≈ 80 nm; Salerno et al., 2018) to coarse (i.e., 162 µm), the strongest peeling forces were measured from roots attached to the smoothest surface tested (i.e., resin replica of glass; Figure 1), indicating that attachment must have been attained by means of adhesive secretions, since there were no asperities present for any mechanical interlocking of root hairs to take place. This result is in contrast to that of a study by Zenone et al. (2020a) with a similar experimental design, in which seagrasses did not attach to a glass replica. In the present study, higher peeling forces were generally measured for roots on smoother substrates (i.e., 0, 0.3, and 12 µm), while roots on the coarser substrates (i.e., 68 and 162 µm) had the weakest peeling forces. These results suggest that substrate microtopography is not a key requirement for the plant to achieve effective attachment to the substrate. No definite conclusion can be drawn from the shear forces since they were not significantly different across the roughness levels and the sample size was too small. Thus, there was no universal mechanism for *Anthurium obtusum* to attach to the substrate. Instead, there seems to be a shift from an adhesive to an

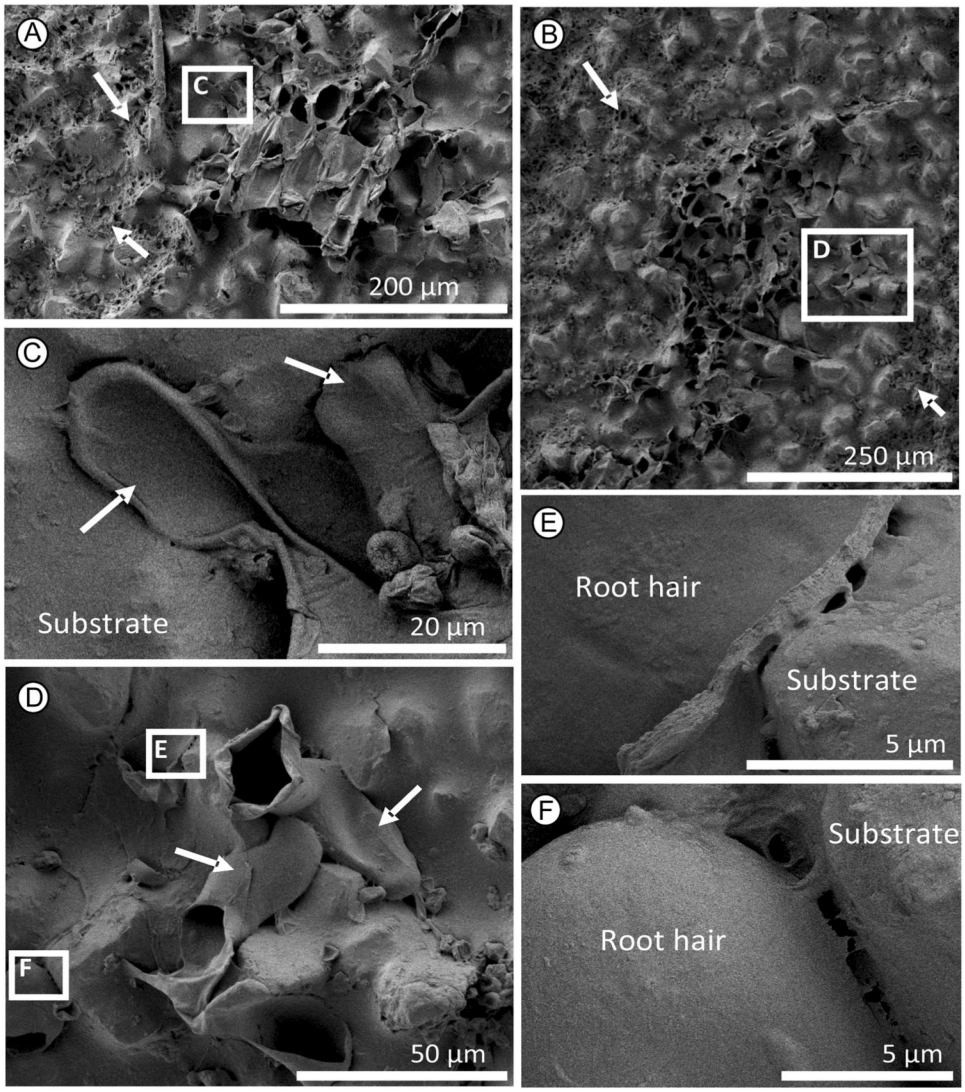

FIGURE 5 Cryo-SEM micrographs of *Anthurium obtusum* with its root hairs adhering to the resin of roughness 30 µm. (A, B) Overview of root piece with the underside attached to the resin, after the root was peeled off the resin. The part to which the root was attached is not overgrown with algae (indicated by white arrows) compared to the areas next to the root. (C, D) Enlargements of boxed areas in (A) and (B), respectively. Root hairs (white arrows) have entered the spaces between the surface asperities, increasing the area of contact to the resin and enhancing attachment strength. (E, F) Enlargements of boxed areas in (D). (E) Thickness of the root hair is ca. 0.45 µm. (F) Some amorphous substance (glue) between the root hair and the resin surface is visible, possibly to aid in adherence of the root.

interlocking mechanism as substrate topography becomes increasingly coarser.

The root hairs had very thin cell walls (Figure 5E), which could have helped the root hairs to adapt and replicate the substrate surface topography. Although root hairs of *A. obtusum* do not branch at the tip, as observed by Zenone et al. (2020a) for *Posidonia oceanica*, they still have a differentiated appearance depending on the roughness of the substrate. An amorphous glue-like substance was observed on the surface of the root hairs and in the root hair–substrate interface (Figures 3E; 4A, D; 5C, E). Our observation of a glue-like substance is not the first for epiphytes. It has been described for epiphytic orchids (Tay et al., 2021) and ferns (Testo and Sundue, 2014). Such a substance has also been observed at the root–substrate interface in numerous attachment systems of climbers and seagrasses (e.g., Darwin, 1867; Groot et al., 2003; Melzer et al., 2011; Steinbrecher et al., 2011; Bohn et al., 2015; Zenone et al., 2020b). For example, aerial roots of *Syngonium podophyllum* secrete a glue-like substance that was a composite of polysaccharides and proteins (Yang and Deng, 2017). Ivy plants secrete nanoparticles from the adhesive disks on the aerial rootlets to affix themselves to a surface (Zhang et al., 2008). These nanoparticles consist mainly of arabinogalactan proteins, which have very low viscosity, allowing effective wetting of the surface by the ivy adhesive (Huang et al., 2016). For seagrasses, Zenone et al. (2020b) hypothesized that the glue could be the first step in

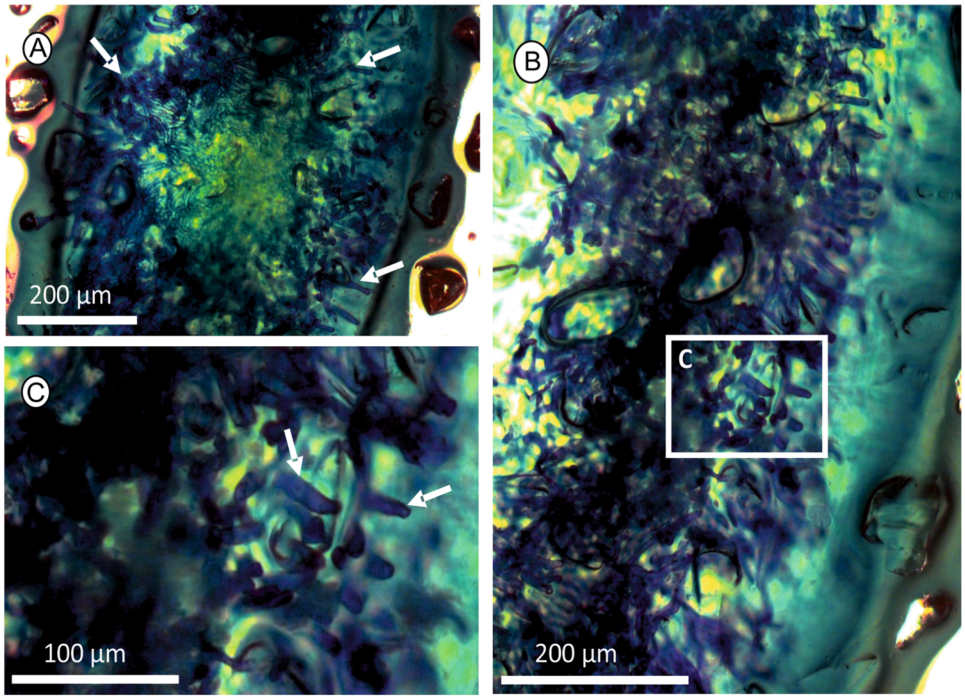

FIGURE 6 Light microscopy images of the underside of the attached root of *Anthurium obtusum* on the surface roughness of 162 µm (highest roughness used in this study). Root hairs are stained with methylene blue and appear blue (some root hairs indicated by arrows). (A) Overview of root hairs that elongated on the substrate. (B) Arrangement of root hairs around the substrate asperities. (C) Root hairs are tubular and seem to wrap around the grains of the rough surface.

securing attachment by facilitating the initial adhesion of the root to the substrate, functioning as a filler to fill the microcrevices of the substrate and enhance real contact area. In this study, the glue-like substance was perhaps sufficient to fill the remaining spaces between root and substrate, especially so on the smoother substrate, hence providing an enlarged contact area responsible for promoting strong adhesion between the root and substrate. As the substrate gets coarser, the glue may not be sufficient to fill increasing larger interface between individual root hairs and between root hairs and substrate. Root hairs were also mostly non-overlapping, tubular-shaped, and do not replicate the substrate surface. Instead, they entered the spaces and achieved contact with the substrate at multiple places (Figure 5D). Therefore, the peeling forces of the root hairs on the coarse substrates are lower since the amount of glue on the root hair is just enough to support the discrete contacts. Nonetheless, another factor influencing the adhesion is the mechanical interlocking of the root hairs to the substrate to promote anchorage, which is observed on coarse substrates. If there was a perfect interlocking of the root hairs to the asperities, the maximum peeling force should be limited by the rupture force of the root hairs. However, our results showed that the peeling force of the aroid seedlings on substrate with increasing roughness did not increase and plateau. The peeling force was instead even decreased at the higher roughness of 68 and 162 µm, suggesting that either the mechanical interlocking for anchorage is limited on very coarse substrates or due to the rupturing of the root hairs (Figure 1).

Anchorage mechanism in the ecological context: bark rugosity

This greenhouse study using artificial substrates provided preliminary findings on how epiphyte roots attach to substrate of different microroughness. In the case of seedling establishment, results from the present study clearly showed that characterising bark rugosity visually and using it as a trait to explain epiphyte occurrences and diversity is inaccurate. The relevant "roughness" for root attachment occurred at the fine microscale of the root-substrate topography. Results showed that aroid seedlings successfully attached to all levels of tested substrate roughness, and these roughness values are at a very different spatial scale from the ones measured on tree bark (e.g., bark roughness ranged between 0.20 and 11.30 cm; Callaway et al., 2002). Thus, the measurement of the outer bark roughness is sometimes irrelevant (unless in the case of a highly rugose bark where the whole root gets lodged into the fissure and obtaining strong attachment). Therefore, previous studies claiming a relationship between "bark roughness" and epiphyte abundance should be viewed with caution, and the exact attachment mechanism of the epiphyte to its host should be clarified.

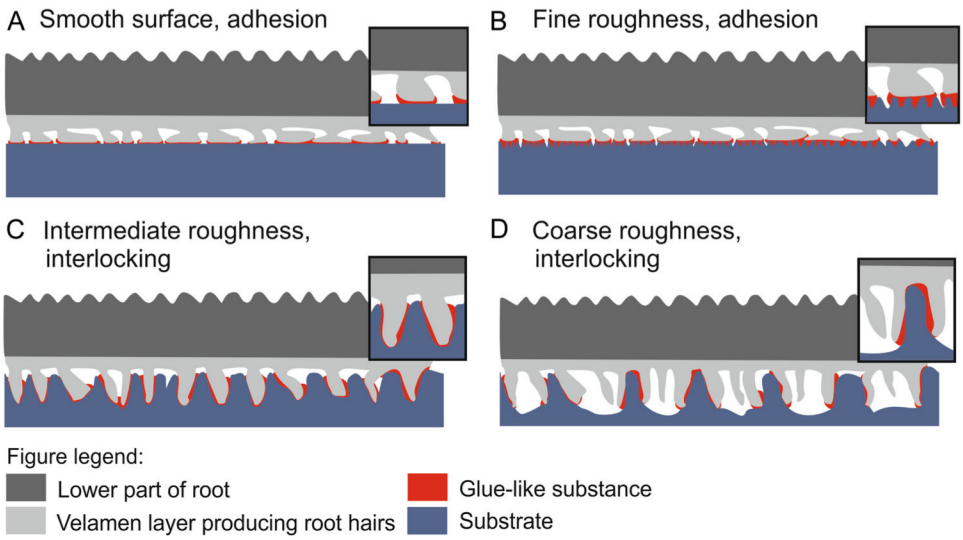

FIGURE 7 Schematic diagram illustrating how epiphytic aroids attach to substrates of varying levels of roughness, as deduced from observations. (A) On smooth surfaces, root hairs are mainly flattened, and the glue-like substance aids in achieving attachment with adhesion. (B) On substrates with fine roughness, roots hairs are still flattened, and the glue-like substance is still sufficient to fill the spaces between the root and substrate to achieve attachment with adhesion. (C) On substrates with intermediate roughness, root hairs are tubular and fit into the microcrevices of the substrate. The glue-like substrate is no longer sufficient for effective attachment; attachment is improved by mechanical interlocking of the root hairs with the substrate. (D) On substrates with coarse roughness, root hairs are too short to achieve sufficient contact with the substrate, but the tubular root hairs grow into the crevices where possible, and attachment is enhanced by mechanical interlocking of the root hairs with the substrate.

Root tensile strength

In the shear test, it is worth noting that on the roughness of 0.3, 3, and 12 μm, the roots mostly detached as a whole, but on the roughness of 0, 30, 68, and 162 μm, the roots were often cut by the thread (Appendix S6). Therefore, the actual shear forces could be greater than what was recorded. On the coarser substrates with roughness of 30, 68, and 162 μm, the phenomenon of the root getting cut by the thread reiterates that although the peeling force is low (due to limited adhesion by glue), mechanical interlocking mechanism between the root hairs and the asperities contributes to the overall anchorage of the plant. Occasionally, the root broke in the middle before it was fully detached from the substrate. In this case, the fracture force of the root itself could be the bottleneck of the system because the root hair–substrate anchorage strength was larger than the innate tensile strength of the root. During the shear test, the shear stress is distributed more or less homogeneous along the whole piece of a root, whereas during the peeling test, the root piece normally bends or acts as a lever, and the mechanical stress is concentrated in a smaller peeling region. Thus, the measured peeling forces are typically less than the shear forces (Figures 1 and 2). In the peel test, at the roughness of 0, 0.3, 3, and 12 μm, root traces often remained on the substrate after the root was peeled off. Therefore, the actual maximum anchorage force should be higher than measured, and again, the root fracture force was the weaker link. The relationship between root–substrate anchorage strength and root tensile strength is important, because they influence one another when the plant experiences external mechanical loads such as wind, rain, self-weight of the plant, and debris or animals on the plant.

CONCLUSIONS

This study on the root attachment mechanism and strength of an epiphytic aroid illustrates that the exact attachment mechanism of *Anthurium obtusum* varies as a function of the substrate microtopography. In the natural environment, epiphytes are found on a wide variety of host trees, differing in texture and surface evenness. Therefore, having combined attachment mechanisms, as described in this study, allow epiphytes to attach effectively to the wide range of their host trees. There are certainly other aspects regarding the attachment mechanism of epiphytes that can be investigated in future studies. For example, this study mainly focused on root attachment mechanics at microroughness scales. However, on a larger scale of the outer bark structure such as deeply fissured bark, the entire root can probably grow directly into the furrows and attach strongly to the host. Therefore, bark rugosity needs to be studied on different scales to fully comprehend the complexity of epiphyte root attachment to different host trees. The glue-like substance observed in this study has neither been systematically analyzed to identify where it is exuded on the root, nor its components quantified. Further studies on these aspects will contribute to molecular and chemical aspects of bio-adhesion systems. Furthermore, it is still unknown how the attachment strength scales with plant size. As the epiphyte grows, it needs to stay attached to its host. Even without additional mechanical disturbances, root attachment has to be

strong enough to support the plant's own weight, withstand gravitational downward force and, in the case of tank bromeliads, the weight of impounded water and organic matter. Mature plants also produce more and thicker roots, that might have different biomechanical properties compared to the young fresh root as measured in this study. Therefore, it will be interesting to investigate how these factors effective anchorage.

Combining insights from previous studies and new observations and experimental data from this study, we summarize our current understanding of how an epiphytic aroid attaches to substrates via their roots and propose mechanisms that this epiphyte might use on substrates that differ from smooth to rough in their surface topography (Figure 7):

(A) On very smooth substrates (i.e., 0 μm roughness), root hairs are flattened on the substrate, which results in a large contact area with the substrate. Attachment is mainly by adhesion with the glue-like substance produced by the root hairs.
(B) On substrates with fine roughness (i.e., 0.3–12 μm roughness), root hairs are also flattened and can replicate the surface topography well. The attachment mechanism is also mainly by adhesion because the glue-like substance produced from the root hairs can fill the nanocrevices of the substrate, thus increasing the actual contact area.
(C) On substrates with intermediate roughness (i.e., 30 μm roughness), the surface topography is more rugged and adhesion via the glue-like substance is no longer sufficient to achieve effective attachment. Root hairs attain a tubular shape and conform to the micro-crevices to attach via mechanical interlocking.
(D) On substrates with coarse roughness (i.e., 68–162 μm roughness), root hairs start to be limited when their short length cannot reach sufficient contact area with the substrate. As the tubular root hairs grow and conform to the crevices, attachment is enhanced by mechanical interlocking when the root hairs clasp the surfaces of the substrate and increase the contact area.

AUTHOR CONTRIBUTIONS

S.G., A.K., and J.T. conceived and designed the research. S.G. contributed analytical tools. J.T. conducted the experiments and analysis, analyzed the data, and wrote the manuscript, with A.K. contributing to the interpretation of the results. G.Z., H.E., A.K., and S.G. revised the manuscript. All authors read and approved the final manuscript.

ACKNOWLEDGMENTS

We thank Dietrich Ober for access to the Botanical Garden Kiel and making their greenhouse available to carry out part of this study and Esther Appel from the Functional Morphology and Biomechanics group in Kiel for guidance in preparing the epoxy resin. We also thank the two reviewers for their comments that improved the manuscript. This work was supported by a grant from the German Research Foundation (Grant number El 1092/1-1) (https://www.dfg.de). Open Access funding enabled and organized by Projekt DEAL.

DATA AVAILABILITY STATEMENT

Data are archived with the FigShare data repository and after a 1-year embargo available from https://doi.org/10.25573/data.19630062.

ORCID

Jessica Y. L. Tay http://orcid.org/0000-0002-5701-4660
Alexander Kovalev http://orcid.org/0000-0002-9441-5316
Gerhard Zotz http://orcid.org/0000-0002-6823-2268
Helena J. R. Einzmann http://orcid.org/0000-0002-4856-3967
Stanislav N. Gorb http://orcid.org/0000-0001-9712-7953

REFERENCES

Adhikari, Y. P., A. Fischer, and H. S. Fischer. 2012. Micro-site conditions of epiphytic orchids in a human impact gradient in Kathmandu valley, Nepal. *Journal of Mountain Science* 9: 331–342.

Badalamenti, F., A. Alagna, and S. Fici. 2015. Evidences of adaptive traits to rocky substrates undermine paradigm of habitat preference of the Mediterranean seagrass *Posidonia oceanica*. *Scientific Reports* 5: 1–6.

Benzing, D. 1970. Roots in certain species of *Tillandsia* and *Vriesea* and their role in the epiphytic environment. *Bulletin of the Bromeliad* Society 20: 79–84.

Blackwell, P., K. Rennolls, and M. Coutts. 1990. A root anchorage model for shallowly rooted Sitka spruce. *Forestry: An International Journal of Forest Research* 63: 73–91.

Bohn, H. F., F. Günther, S. Fink, and T. Speck. 2015. A passionate free climber: structural development and functional morphology of the adhesive tendrils in *Passiflora discophora*. *International Journal of Plant Sciences* 176: 294–305.

Borgin, K., and K. Corbett. 1971. The hydrophobic properties of bark extractives. *Wood Science and Technology* 5: 190–199.

Borgin, K., and K. Corbett. 1974. The hydrophobic and water-repellent properties of wattle bark extractives. *Wood Science and Technology* 8: 138–147.

Borovec, O., and M. Vohník. 2018. Ontogenetic transition from specialized root hairs to specific root-fungus symbiosis in the dominant Mediterranean seagrass *Posidonia oceanica*. *Scientific Reports* 8: 1–11.

Brandt, F. B., G. O. Martinson, and R. Conrad. 2017. Bromeliad tanks are unique habitats for microbial communities involved in methane turnover. *Plant and Soil* 410: 167–179.

Brighigna, L., A. C. Fiordi, and M. Palandri. 1990. Structural comparison between free and anchored roots in *Tillandsia* (Bromeliaceae) species. *Caryologia* 43: 27–42.

Callaway, R. M., K. O. Reinhart, G. W. Moore, D. J. Moore, and S. C. Pennings. 2002. Epiphyte host preferences and host traits: mechanisms for species-specific interactions. *Oecologia* 132: 221–230.

Ceballos, S. J., N. P. Chacoff, and A. Malizia. 2016. Interaction network of vascular epiphytes and trees in a subtropical forest. *Acta Oecologica* 77: 152–159.

Coutts, M. 1983. Root architecture and tree stability. *In* D. Atkinson, K. K. S. Bhat, M. P. Coutts, P. A. Mason, and D. J. Read [eds.], Tree root systems and their mycorrhizas, 171–188. Springer, Dordrecht, Netherlands.

Coutts, M. 1986. Components of tree stability in Sitka spruce on peaty gley soil. *Forestry* 59: 173–197.

Crook, M., and A. Ennos. 1996. The anchorage mechanics of deep rooted larch, *Larix europea* × *L. japonica*. *Journal of Experimental Botany* 47: 1509–1517.

Crook, M., A. Ennos, and J. Banks. 1997. The function of buttress roots: a comparative study of the anchorage systems of buttressed (*Aglaia* and *Nephelium ramboutan* species) and non-buttressed (*Mallotus wrayi*) tropical trees. *Journal of Experimental Botany* 48: 1703–1716.

Darwin, C. 1867. The movements and habits of climbing plants. *Journal of the Linnean Society of Botany* 9: 1–118.

Deseo, N. B., C. C. De Guzman, P. A. Nuevo, and N. K. Torreta. 2020. Morpho-anatomy of adventitious roots of vanilla (*Vanilla planifolia* Jacks. ex Andrews) during attachment to support post. *Thailand Natural History Museum Journal* 14: 31–36.

Di Iorio, A., B. Lasserre, G. S. Scippa, and D. Chiatante. 2004. Root system architecture of *Quercus pubescens* trees growing on different sloping conditions. *Annals of Botany* 95: 351–361.

Drelich, J., E. Chibowski, D. D. Meng, and K. Terpilowski. 2011. Hydrophilic and superhydrophilic surfaces and materials. *Soft Matter* 7: 9804–9828.

Dupuy, L., T. Fourcaud, and A. Stokes. 2007. A numerical investigation into the influence of soil type and root architecture on tree anchorage. *In* A. Stokes, I. Spanos, J. E. Norris, and E. Cammeraat [eds.], Eco-and ground bio-engineering: the use of vegetation to improve slope stability, 175–189. Springer, Dordrecht, Netherlands.

Dycus, A. M., and L. Knudson. 1957. The role of the velamen of the aerial roots of orchids. *Botanical Gazette* 119: 78–87.

Ennos, A. 1989. The mechanics of anchorage in seedlings of sunflower, *Helianthus annuus* L. *New Phytologist* 113: 185–192.

Ennos, A. 1990. The anchorage of leek seedlings: the effect of root length and soil strength. *Annals of Botany* 65: 409–416.

Ennos, A. 1993. The function and formation of buttresses. *Trends in Ecology & Evolution* 8: 350–351.

Ennos, A. 2000. The mechanics of root anchorage. *Advances in Botanical Research* 33: 133–157.

Ennos, A., and A. Fitter. 1992. Comparative functional morphology of the anchorage systems of annual dicots. *Functional Ecology* 6: 71–78.

Fourcaud, T., F. Danjon, and L. Dupuy. 2003. Numerical analysis of the anchorage of Maritime pine trees in connection with root structure. *In* B. Ruck, C. Kottmeier, C. Mattheck, C. Quine, and G. Wilhelm [eds.], Proceedings of the international conference Wind Effects on Trees, 323–330. Karlsruhe University, Karlsruhe, Germany.

Fournier, M., A. Stokes, C. Coutand, T. Fourcaud, and B. Moulia. 2006. Tree biomechanics and growth strategies in the context of forest functional ecology. *In* A. Herrel, T. Speck, and N. P. Rowe [eds.], Ecology and biomechanics–a mechanical approach to the ecology of animals and plants, 1–34. Taylor & Francis Group Boca Raton, FL, USA.

Gartner, B. L. 1994. Root biomechanics and whole-plant allocation patterns: responses of tomato plants to stem flexure. *Journal of Experimental Botany* 45: 1647–1654.

Groot, E. P., E. J. Sweeney, and T. L. Rost. 2003. Development of the adhesive pad on climbing fig (*Ficus pumila*) stems from clusters of adventitious roots. *Plant and Soil* 248: 85–96.

Hietz, P., and U. Hietz-Seifert. 1995. Composition and ecology of vascular epiphyte communities along an altitudinal gradient in central Veracruz, Mexico. *Journal of Vegetation Science* 6: 487–498.

Hoeber, V., T. Weichgrebe, and G. Zotz. 2019. Accidental epiphytism in the Harz Mountains, Central Europe. *Journal of Vegetation Science* 30: 765–775.

Huang, Y., Y. Wang, L. Tan, L. Sun, J. Petrosino, M. Cui, F. Hao, and M. Zhang. 2016. Nanospherical arabinogalactan proteins are a key component of the high-strength adhesive secreted by English ivy. *Proceedings of the National Academy of Sciences, USA* 113: E3193–E3202.

Isnard, S., and W. K. Silk. 2009. Moving with climbing plants from Charles Darwin's time into the 21st century. *American Journal of Botany* 96: 1205–1221.

Lewis, J. E., and C. J. Ellis. 2010. Taxon-compared with trait-based analysis of epiphytes, and the role of tree species and tree age in community composition. *Plant Ecology & Diversity* 3: 203–210.

Malizia, A. 2003. Host tree preference of vascular epiphytes and climbers in a subtropical montane cloud forest of Northwest Argentina. *Selbyana* 24: 196–205.

Matelson, T. J., N. M. Nadkarni, and J. T. Longino. 1993. Longevity of fallen epiphytes in a neotropical montane forest. *Ecology* 74: 265–269.

Mathews, M., M. L. Wee, and K. K. Ho. 1997. Growth and development of aerial roots of a tropical ornamental, *Philodendron lacerum*. *Journal of Horticultural Science* 72: 27–34.

Melzer, B., R. Seidel, T. Steinbrecher, and T. Speck. 2011. Structure, attachment properties, and ecological importance of the attachment system of English ivy (*Hedera helix*). *Journal of Experimental Botany* 63: 191–201.

Mickovski, S. B., and A. R. Ennos. 2003. Anchorage and asymmetry in the root system of *Pinus peuce*. *Silva Fennica* 37: 161–173.

Muthukumar, T., and A. Kowsalya. 2017. Comparative anatomy of aerial and substrate roots of *Acampe praemorsa* (Rox.) Blatt. & McCann. *Flora* 226: 17–28.

Nicoll, B. C., B. A. Gardiner, B. Rayner, and A. J. Peace. 2006. Anchorage of coniferous trees in relation to species, soil type, and rooting depth. *Canadian Journal of Forest Research* 36: 1871–1883.

Nicoll, B. C., and D. Ray. 1996. Adaptive growth of tree root systems in response to wind action and site conditions. *Tree Physiology* 16: 891–898.

Oliver, W. R. B. 1930. New Zealand epiphytes. *Journal of Ecology* 18: 1–50.

Passialis, C. N., and E. V. Voulgaridis. 1999. Water repellent efficiency of organic solvent extractives from Aleppo pine leaves and bark applied to wood. *Wood Research and Technology: Holzforschung* 53: 151–155.

Peltola, H., S. Kellomäki, A. Hassinen, and M. Granander. 2000. Mechanical stability of Scots pine, Norway spruce and birch: an analysis of tree-pulling experiments in Finland. *Forest Ecology and Management* 135: 143–153.

Ponert, J., P. Trávníček, T. B. Vuong, R. Rybková, and J. Suda. 2016. A new species of *Cleisostoma* (Orchidaceae) from the Hon Ba Nature Reserve in Vietnam: a multidisciplinary assessment. *PLoS One* 11: e0150631.

R Core Team. 2021. R: a language and environment for statistical computing. R Foundation for Statistical Computing, Vienna, Austria. Website: http://www.R-project.org

Rodríguez-Robles, J. A., J. D. Ackerman, and E. Meléndez. 1990. Host distribution and hurricane damage to an orchid population at Toro Negro Forest, Puerto Rico. *Caribbean Journal of Science* 26: 163–164.

Rudolph, D., G. Rauer, J. Nieder, and W. Barthlott. 1998. Distributional patterns of epiphytes in the canopy and phorophyte characteristics in a western Andean rain forest in Ecuador. *Selbyana* 19: 27–33.

Salerno, G., M. Rebora, A. Kovalev, E. Gorb, and S. Gorb. 2018. Contribution of different tarsal attachment devices to the overall attachment ability of the stink bug *Nezara viridula*. *Journal of Comparative Physiology A* 204: 627–638.

Schimper, A. F. W. 1888. Die epiphytische vegetation Amerikas. G. Fischer, Jena, Germany.

Schindelin, J., I. Arganda-Carreras, E. Frise, V. Kaynig, M. Longair, T. Pietzsch, S. Preibisch, et al., 2012. Fiji: an open-source platform for biological-image analysis. *Nature Methods* 9: 676–682.

Steege, H. T., and J. H. C. Cornelissen. 1989. Distribution and ecology of vascular epiphytes in lowland rain forest of Guyana. *Biotropica* 21: 331–339.

Steinbrecher, T., G. Beuchle, B. Melzer, T. Speck, O. Kraft, and R. Schwaiger. 2011. Structural development and morphology of the attachment system of *Parthenocissus tricuspidata*. *International Journal of Plant Sciences* 172: 1120–1129.

Steinbrecher, T., E. Danninger, D. Harder, T. Speck, O. Kraft, and R. Schwaiger. 2010. Quantifying the attachment strength of climbing plants: a new approach. *Acta Biomaterialia* 6: 1497–1504.

Stern, W. L. 2014. Anatomy of the monocotyledons, vol. X, Orchidaceae. Oxford University Press, Oxford, UK.

Stern, W. L., and W. S. Judd. 1999. Comparative vegetative anatomy and systematics of *Vanilla* (Orchidaceae). *Botanical Journal of the Linnean Society* 131: 353–382.

Štofko, P., and M. Kodrik. 2008. Comparison of the root system architecture between windthrown and undamaged spruces growing in poorly drained sites. *Journal of Forest Science* 54: 150–160.

Stokes, A. 1999. Strain distribution during anchorage failure of *Pinus pinaster* Ait. at different ages and tree growth response to wind-induced root movement. *Plant and Soil* 217: 17–27.

Stokes, A., and D. Guitard. 1997. Tree root response to mechanical stress. *In*: A. Altman and Y. Waisel [eds.], Biology of root formation and development, 227–236. Springer, Boston, MA, USA.

Tay, J. Y., G. Zotz, and H. J. Einzmann. 2022. Thigmomorphogenic responses of epiphytic bromeliads to mechanically induced stress. *Plant Ecology* 223: 1–11.

Tay, J. Y., G. Zotz, S. N. Gorb, and H. J. Einzmann. 2021. Getting a grip on the adhesion mechanism of epiphytic orchids–evidence from histology and cryo-scanning electron microscopy. *Frontiers in Forests and Global Change* 4: 764357.

Telewski, F. 1995. Wind-induced physiological and developmental responses in trees. *In:* J. Grace and M. P. Coutts [eds.], Wind and trees, 237–263. Cambridge University Press, Cambridge, UK.

Testo, W., and M. Sundue. 2014. Primary hemiepiphytism in *Colysis ampla* (Polypodiaceae) provides new insight into the evolution of growth habit in ferns. *International Journal of Plant Sciences* 175: 526–536.

Tremblay, R. L. 2008. Ecological correlates and short-term effects of relocation of a rare epiphytic orchid after Hurricane Georges. *Endangered Species Research* 5: 83–90.

Van Leerdam, A., R. Zagt, and E. Veneklaas. 1990. The distribution of epiphyte growth-forms in the canopy of a Colombian cloud-forest. *Vegetatio* 87: 59–71.

Voigt, D., S. Gorb, and J.-L. Boevé. 2011. Superhydrophobic cuticle with a "pinning effect" in the larvae of the iris sawfly, *Rhadinoceraea micans* (Hymenoptera, Tenthredinidae). *Zoology* 114: 265–271.

Warren, S. D., H. L. Black, D. A. Eastmond, and W. H. Whaley. 1988. Structural function of buttresses of *Tachigalia versicolor*. *Ecology* 69: 532–536.

WCSP. 2022. World checklist of selected plant families [online]. Facilitated by the Royal Botanic Gardens, Kew, UK. Website: http://wcsp.science.kew.org

Went, F. W. 1940. Soziologie der Epiphyten eines tropischen Urwaldes. E. J. Brill, Leiden, Netherlands.

Wyse, S. V., and B. R. Burns. 2011. Do host bark traits influence trunk epiphyte communities? *New Zealand Journal of Ecology* 35: 296–301.

Yang, X., and W. Deng. 2017. Morphological and structural characterization of the attachment system in aerial roots of *Syngonium podophyllum*. *Planta* 245: 507–521.

Zenone, A., A. Alagna, G. D'anna, A. Kovalev, A. Kreitschitz, F. Badalamenti, and S. N. Gorb. 2020a. Biological adhesion in seagrasses: the role of substrate roughness in *Posidonia oceanica* (L.) Delile seedling anchorage via adhesive root hairs. *Marine Environmental Research* 160: 105012.

Zenone, A., A. Filippov, A. Kovalev, F. Badalamenti, and S. N. Gorb. 2020b. Root hair adhesion in *Posidonia oceanica* (L.) Delile seedlings: a numerical modelling approach. *Frontiers in Mechanical Engineering* 6: 590894.

Zhang, M., M. Liu, H. Prest, and S. Fischer. 2008. Nanoparticles secreted from ivy rootlets for surface climbing. *Nano Letters* 8: 1277–1280.

Zotz, G., P. Hietz, and H. J. R. Einzmann. 2021a. Functional ecology of vascular epiphytes. *Annual Plant Reviews Online* 4: 869–906.

Zotz, G., M. Leja, Y. Aguilar-Cruz, and H. J. Einzmann. 2020. How much water is in the tank? An allometric analysis with 205 bromeliad species. *Flora* 264: 151557.

Zotz, G., P. Weigelt, M. Kessler, H. Kreft, and A. Taylor. 2021b. EpiList 1.0: a global checklist of vascular epiphytes. *Ecology* 102: e03326.

SUPPORTING INFORMATION

Additional Supporting Information may be found online in the supporting information section at the end of the article.

Appendix S1. Example of a *Tillandsia subulifera* attached to a twig. The roots are attached to the twig, and not covered with any organic material.

Appendix S2. Resin tiles with seedlings held in place with rubber bands. The tiles were randomized spatially every week. Seedlings were left to grow on the tiles for 2 months.

Appendix S3. Examples of resin tiles of different surface roughness with 2-month-old seedlings growing on them. Scale = 3 cm.

Appendix S4. Setup for anchorage strength measurement. The tile was fixed onto the test platform with double-sided tape. One end of a nylon thread was tied to the cut end of the root (cut at the proximal end with a disposable razor blade), and the other end was fixed to the sensor of the tester. (A) The sensor was positioned at 90° to the tile surface for the peel test and (B) at 0° to the tile surface for the shear test (root was dyed with methylene blue).

Appendix S5. Light micrographs of the underside of the attached root of *Anthurium obtusum* on different levels of surface roughness. (A) Root had a tight contact with the resin tile, preventing methylene blue from staining the root hairs sufficiently. Root hairs were still clearly visible as extensions from the velamen layer (a single root hair is highlighted red). (B, C) Root hairs were visible from the sides of root. The number on the bottom-right of each image indicates the roughness of the resin tile. All scale bars = 200 µm.

Appendix S6. Shear test of a root on a tile of roughness 30 µm. Root was not detached from the tile as a whole, but instead got cut by the thread. Root was dyed with methylene blue.

How to cite this article: Tay, J. Y. L., A. Kovalev, G. Zotz, H. J. R. Einzmann, and S. N. Gorb. 2022. Holding on or falling off: The attachment mechanism of epiphytic *Anthurium obtusum* changes with substrate roughness. *American Journal of Botany* 109(6): 874–886. https://doi.org/10.1002/ajb2.16000